Vol. 38, No. 1 (2016) 49-59

Tribology in Industry

www.tribology.fink.rs

RESEARCH

COMPARISON OF MECHANICAL PROPERTIES IN COMPACTED AND SPHEROIDAL GRAPHITE IRONS

Cristiano Fragassa, Nenad Radovic, Ana Pavlovic, Giangiacomo Minak

Department of Industrial Engineering, Alma Mater Studiorum University of Bologna

Keywords:

Cast Iron; Foundry; Tensile Test; Experimental Tests; Mechanical Resistances; Microstructures.

Corresponding author:

Cristiano Fragassa
University of Bologna,
viale Risorgimento 2, Bologna, Italy
E-mail: cristiano.fragassa@unibo.it

A B S T R A C T

Mechanical properties of cast irons are governed by the size, distribution and shape of the incorporated graphite particles. In a set of experiments, two groups of cast alloys, Compacted Graphite Iron (CGI) and Spheroidal Graphite Iron (SGI) were investigated. Even if the processes used for their production could be apparently considered quite similar, these two materials are characterized by a net difference in graphite particles and, as consequence, in final properties. Adding, while SGI benefits of a wide scientific literature supporting its large use, CGI is a relatively unexplored.

1. INTRODUCTION

Until the 19th century, cast iron was commonly defined as "scrap steel" for its low quality and workability compared to mild steel. For some time now, the cast iron is better known as a very useful and multipurpose ferrous metal alloy, characterized by a relatively high content of carbon [1]. This Fe-C alloy, also including secondary elements, presents a carbon content between 1.9% and 5.5%, up to the saturation limit of 6.67%. Its production is usually realized by a process of reduction of iron oxides by coal combustion in contact with iron inside the blast furnaces. The ore is disposed with alternating layers of coal. Coal, typically coke, has a low sulfur content. The iron in the ore, in the molten state, drains down in appropriate containers. This cast iron is said “of first melting” or “untreated” and used to produce the "industrial" steel [2-3]. This steel is recast, either directly or after removal or addition of other elements such as silicon, manganese, sulfur, phosphorus. The material is poured into molds in foundry processes for casting metal industry (Figs. 1, 2). More broadly, the cast iron is a material hard and brittle, weak in tensile and bending, but very made-existing in compression and corrosion. Since its high malleability, this material is not an appropriate solution when plastic deformations occur, neither hot nor cold. On the contrary, it presents a good fusibility represented by a not very high melting temperature. Adding, it has a good fluidity when melted, which leads to "healthy" and compact castings. It allows an easy realization of cast pieces even in the case of complex geometries. Furthermore, the cast irons may present physical characteristics very variable based on metal texture, shape and volume of the graphite, the production process and any heat treatment [4-5]. The levels relatively high silicon guarantee good resistance to oxidation, corrosion [6] and wear [7], contributing to the long life of the components.

Fig. 1. Production of cast iron in laboratory

Fig. 2. Production of cast iron in factory (courtesy US Navy)

The family of cast irons consists of [4-5]:

grey cast iron (or *lamellar*): characterized by graphite in the form of lamellae (Fig. 3a), has excellent castability, machinability, high hardness and wear resistance and excellent damping properties of the vibration. Placing a unitary damping capacity for the grey cast iron, the same properties is approximately 0.35 for compacted graphite iron, 0.14 for ductile iron, 0.040 for steel and 0.005 of aluminum. Grey cast iron is therefore optimal, for example, for the production of engine blocks, brake components and bases of machine tools. It is also used for the production of components for boilers, heaters and valves. It is not advisable to use when it is necessary to obtain castings with high tensile strength, as the sheets of graphite, since it promotes the generation of cracks;

spheroidal graphite iron (*ductile*, *nodular,* or briefly ***SGI***): characterized by the presence of graphite in the form of spherical nodules, immersed in a metal matrix, whose structure is a function of the chemical composition, the cooling rate and any subsequent heat treatments (Fig. 3b). The spheroidal shape of the graphite produces a lower stress concentration than the lamellar. Adding, the sphere is the form that presents the lower surface with equal volume: the metal matrix is less damaged allowing a better exploit of features. In particular, the spheroidal cast iron in the graphite nodules exerts a stop for the cracks unlike the lamellar graphite which offers a preferential way for their propagation. Consequently, nodular cast iron presents a significant improvement of all the mechanical characteristics further adding ductility. Common uses for the SGI relates to transportation and machinery for agriculture;

compacted graphite iron (or *vermicular,* briefly ***CGI***) has characteristics interMeante between those of grey iron and ductile iron. The shape of the elements of graphite is called "vermicular" (Fig. 3c). The compacted graphite iron combines the castability and the thermal conductivity of grey cast iron with its properties of strength and stiffness closer to those of ductile iron. Increasing the size of the graphite elements is possible to increase the absorption of vibrations, at the expense of the modulus of elasticity. This cast iron is promising respect to future applications [8]: currently, beyond few interesting attempts, as [9-11], there are no large-scale industrial use. It depends to the fact that the process for manufacturing components in vermicular graphite iron still does not present the necessary reliability and repeatability;

white cast iron: is a particular variety of hard cast iron, and essentially free of graphite, since the carbon in the cast iron is combined largely, if not completely, with the iron, generating cementite (Fig. 3d). White cast iron, that presents silvery fracture, has a very high hardness (up to 500 Brinell), wear and abrasion resistance, but is considerably brittle and not workable tool. White cast iron, often linked with chromium or nichel-crome, is only used for castings which are to withstand very difficult working conditions as high temperatures, high wear or corrosion, as carriage wheels or rolling cylinders.

malleable cast iron: obtained from a white cast iron by an additional heat treatment, presents flocs of graphite of irregular shape which give an excellent malleability, comparable to that of steels (Fig. 3e). It is optimal for the production of small components that require ductility and is the cast iron easier to work by machine tools; however, this alloy is rapidly declining, replaced for the most part by ductile iron, which has similar properties without the mandatory heat treatment. Used primarily in the fields of agriculture, railway and hydraulic motor.

A brief summary about composition, properties and common applications for these families of cast iron is reported in Tab. 1 and 2.

Table 1. Nominal composition and common use of cast irons [12]

Cast Iron	Composition % by weight	Applications
Grey	C 3.4, Si 0.8, Mn 0.5	Engine cylinder blocks, flywheels, gearbox cases, machine-tool bases
Ductile	C 3.4, P 0.1, Mn 0.4, Ni 1.0, Mg 0.06	Gears, camshafts, crankshafts
Compacted	*(similar to ductile)*	-
White	C 3.4, Si 0.7, Mn 0.6	Bearing surfaces
Malleable	C 2.5, Si 1.0, Mn 0.55	Axle bearings, track wheels, automotive crankshafts

As said, the cast irons may present physical properties very variable (tab. 2). For example, the tensile strength may vary from 124 to 1600 MPa. Instead to represent a limit, this variability is a real opportunity of application for this material. For instance, by special attentions, it is possible to obtain a cast iron with high resilience, even at low temperatures, coupled with a moderate resistance, or, vice versa, a alloy with high strength and low values of elongation coupled with high resilience. This flexibility allows the use of cast iron for the realization of components optimized in the case of different functions and or working conditions (tab. 1).

Table 2. Mechanical properties of cast irons [12]

Cast Iron	Yield Strenght [MPa]	Tensile Strenght [MPa]	Elongation %	Brinell Hardness
Grey	-	345	0.5	260
Ductile	745	930	5	310
Compacted	365	480	18	170
White	-	170	0	450
Malleable	230	360	12	130

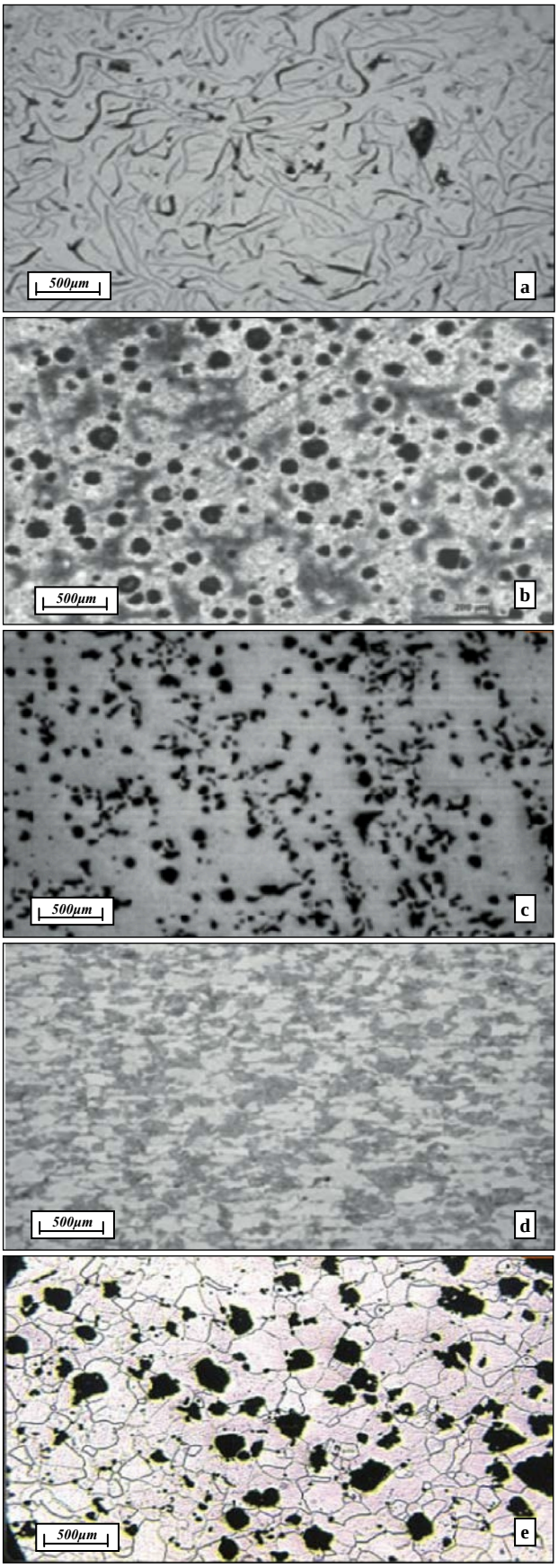

Fig. 3. Comparing cast iron by micrographs: a) grey cast iron; b) ductile iron; c) compacted graphite iron; d) white cast iron; e) malleable cast iron.

2. MATERIALS AND METHODS

2.1 Specimens

In this investigation, several specimens were tested using tensile experiments. The specimens were extracted from CGI and SGI cast plates realized in sand casting (Fig. 4).

Fig. 4. Production of specimens by sand casting in sand casting foundry [13]

It is a metal casting process characterized by using sand as the mould material. Over 70% of all metal castings are produced via a sand casting process, passing by the main phases of:

- ✓ Melting: takes place in a cupola furnace, with layers of coke and ignited with torches. When the coke is ignited, air is introduced to the coke bed through tuyeres in the sides, and when the coke is very hot, solid pieces of metal are charged into the furnace.
- ✓ Moulding: implemented by exploiting the imprint left by the two halves of the pattern on the green sand that fills the lower and upper box.
- ✓ Pouring: the shapes are placed on the pouring line ready to be filled with molten iron.
- ✓ Castings: the molten iron is cast and take the shape needed

Specifically, a plate in SGI and, just after, a plate in CGI were casted. They were realized inside the same process and using, as base, the same melting alloy, but modifying the composition by inclusion of additives. In practice, specific and different additives were directly introduced in the furnace to produce SGI or CGI [14-15]. In the case of SGI castings, before the pouring, the melt (with a sulphur content lower than *0.01% wt.*) was inoculated by adding ferrosilicon alloys and modified with *Fe-Si-Mg* master alloys. In the production of CGI castings also Ti was added.
Special attentions were adopted to keep unchanged the other process conditions, passing from SGI to CGI, and, in particular, the same pouring temperature, fixed at 1400°C.

2.2 Tensile tests

Tensile testing, also known as tension testing, is a fundamental materials science test in which a sample is subjected to uniaxial tension until failure. The results are commonly used to select a material for an application, for quality control, and to predict how a material will react under other configuration of forces.
Material properties directly measured via tensile tests are:

- Ultimate Tensile Strength;
- Maximum Elongation to Failure;
- Reduction in Area;

also determining the additional properties:

- Young's modulus;
- Poisson's ratio;
- Yield strength;
- Strain-hardening characteristics.

Tensile tests were carried out on the uniaxial loading tensile servo-hydraulic testing machine INSTRON® 1343 (Fig. 5).
They were realized according to the EN 10002-1 standard [16], where a procedure for the tensile testing of metallic materials at ambient temperature is described. In particular, these tests used “tensile samples”, with standardized dimensions and shapes.

Fig. 5. Uniaxial loading tensile servo-hydraulic testing machine INSTRON® 1343

A tensile specimen is a standardized sample with two shoulders and a gauge section in between (Fig. 6). The shoulders are large enough to be readily gripped, whereas the gauge section has a smaller cross-section so that the deformation and failure can occur in this area.

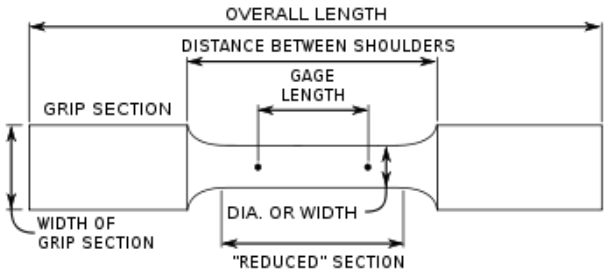

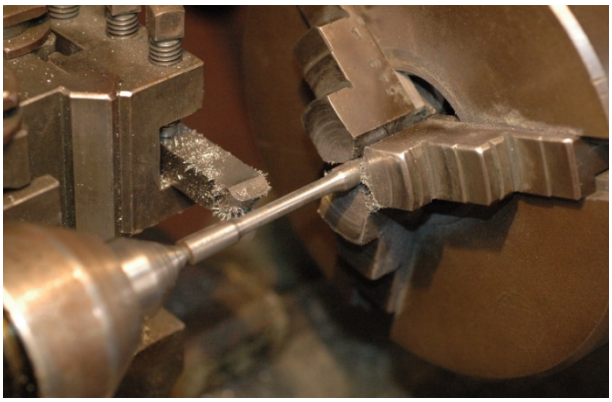

Fig. 6. "Dog bone" shape for a tensile specimen

The "dog bone" shape was machined according to the EN 1563, the European standard for spheroidal graphite cast iron [17]. It outlines legal and regulatory requirements as well as industry grades for materials – providing ways to classify the quality and hardness of spheroidal cast irons. Its specifications are based on the mechanical properties of machine tested materials.

2.3 True Stress vs Engineering Stress

During the experiments, values as "true" and "engineering" stresses were both considered.
Engineering stress assumes that the area a force is acting upon remains constant during the test. This value does not take in count that, during tests, while the length increases, the width and thickness shrink changing the cross area.
The *real stress* takes into account the variation in the cross sectional area as a result of the stress induced deformation (strain) of a material.

To calculate the engineering stress, the applied load is divided by the original cross sectional area. On the contrary, the true stress is equal to the same load divided by the new deformed cross sectional area.
Unless thickness and width are being monitored continuously during the test, it is not possible to calculate true stress. In circle grid analysis, engineering strain is the % expansion of the circle compared to the initial diameter of the circle.
The relationships between engineering values and true values are [18]:

$$\sigma = s\,(1+e)\,. \tag{1}$$

$$\varepsilon = \ln\,(1+e)\,. \tag{2}$$

where "s" and "e" are the engineering stress and strain, respectively, and " σ " and "ε" are the true stress and strain, respectively.
In terms of *true stress*, the stress-strain diagram stops to show a maximal respect to the yield stress providing a constant increase (Fig. 7) in line with a constant increase of the testing load.

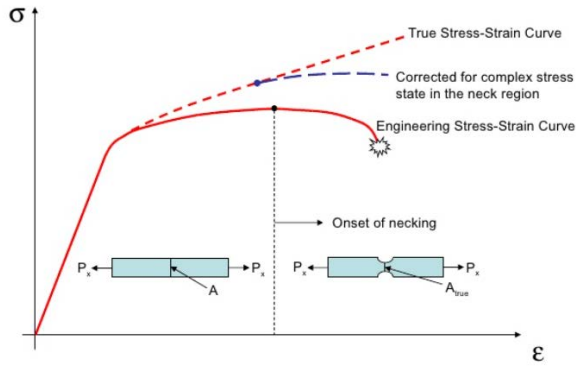

Fig. 7. Stress-strain curve in the case of true stresses and engineering stresses.

The *true stress* is, however, a much better representation of how the material behaves as it is being deformed, which explains its alternative name of "real" stress. This denomination refers to the fact that this stress represents what is the real level of stress "suffered" by the material. True stress is likely to be significantly higher than engineering stress.
Several researches, investigates the difference of real and engineering stress, in general terms [19], or also on practical cases [20].

3. RESULTS

3.1 Experimental data

By EN 10002 tests N. 50 specimens were fully characterized for tensile behaviour, N. 23 in CGI and N. 27 in SGI.
For each specimen the value of

- Ultimate Tensile Strength [UTS];
- Yield Strength [YS].
- Maximal Elongation to Failure[ε];
- Young's modulus [E];

was evaluated as reported in Tab. 3 and 4.
A test for hardness and a chemical analysis regarding some microstructural aspects were also realized and reported in the same tables for a better comparison of specimens.

The experimental values, even at the level of mean values (Tab. 5), confirmed the general concept that SGI is more ductile than CGI. Specifically SGI ultimate tensile strength (549 MPa) is significantly higher than CGI one (337 MPa), around +38%. The same happens for the yield strength, 339 MPa for SGI against 267 MPa of CGI, around +21%. The higher ductility is even better demonstrated by consideration on the maximal elongation before failure: while SGI permits a 10.2% of deformation, 3.4%. is the maximum for CGI. Also the Young's modules for the two irons, with values around 12% higher in the case of SGI, confirm the same trend even if with a lower evidence.

Table 3. Mechanical properties of specimens in Compacted Graphite Iron (CGI)

Specimen	Graphite [%]	Ferrite [%]	Perlite [%]	Grade of Nodularity	Grade of Vermicularity	UTS [MPa]	YS [MPa]	ε [%]	HB	E [GPa]
1	21.0	60.2	18.8	16.1	81.2	318.8	253.1	3.3	136.0	136.1
2	17.3	62.3	20.4	12.1	85.1	350.1	274.3	2.2	139.0	182.5
3	13.9	62.9	23.2	15.4	82.2	307.5	237.8	3.3	142.0	146.3
4	14.5	61.6	23.9	9.4	88.5	314.1	252.4	2.2	145.0	137.1
5	14.5	62.6	22.9	23.4	74.3	316.2	259.1	2.5	144.0	142.1
6	13.2	64.8	22.0	13.0	84.4	308.4	252.3	2.4	144.0	140.8
7	15.7	64.3	20.0	17.5	79.7	321.7	258.5	3.4	141.0	151.4
8	12.6	61.9	25.6	11.7	86.4	315.0	249.7	2.7	137.0	152.9
9	16.7	53.5	29.8	9.0	88.9	312.4	249.5	3.6	132.0	156.3
10	14.9	65.7	19.5	22.1	75.0				137.0	
11	11.4	64.9	23.7	15.1	82.7	338.3	273.0	4.4	151.0	175.6
12	9.2	67.6	23.3	21.6	74.6	338.8	257.3	4.2	156.0	146.4
13	8.5	63.8	27.7	17.8	80.7				151.0	
14	11.2	65.8	22.9	17.9	80.0	336.8	274.0	4.6	142.0	132.1
15	10.3	63.0	26.8	16.7	81.4	339.2	270.9	4.2	147.0	145.7
16	14.6	56.6	28.9	19.5	78.5	345.8	263.9	3.4	146.0	145.8
17	10.1	62.9	27.0	16.7	81.7	346.4	278.4	3.7	147.0	159.2
18	11.1	63.5	25.5	16.2	81.8	354.6	288.3	3.1	150.0	165.6
19	9.8	59.9	30.3	17.8	80.5	345.0	274.9	3.4	151.0	152.6
20	12.8	58.3	28.9	24.0	74.0	345.7	284.1	3.2	149.0	129.8
22	12.9	52.9	34.2	18.5	79.5	370.7	281.0	3.9	150.0	144.3
23	12.6	53.4	34.0	16.3	81.9	374.0	295.8	3.4	148.0	137.9
24	9.7	55.2	35.2	13.3	85.4	380.8	296.7	3.9	147.0	167.9
Mean	**13.0**	**61.2**	**25.8**	**16.6**	**81.2**	**337.2**	**267.9**	**3.4**	**144.9**	**149.9**
St. Dev.	**3.0**	**4.3**	**4.7**	**4.0**	**4.2**	**21.8**	**16.3**	**0.7**	**5.9**	**14.0**

Table 4. Mechanical properties of specimens in Spheroidal Graphite Iron (SGI)

Specimen	Graphite [%]	Ferrite [%]	Perlite [%]	Grade of nodularity	Grade of Vermicularity	UTS [MPa]	YS [MPa]	ε [%]	HB	E [GPa]
25	9,1	47,5	43,4	53,9	36,8	500,0	315,3	10,2	173,0	154,5
26	12,2	47,1	40,8	63,6	27,2	501,0	302,3	10,3	171,0	164,6
27	13,6	42,5	43,9	75,2	17,0	508,7	315,7	8,6	165,0	184,9
28	8,6	48,6	42,8	62,6	30,4	496,8	301,2	11,6	171,0	184,9
29	12,1	48,5	39,5	67,1	26,2	494,8	325,4	8,5	168,0	170,5
30	11,2	42,8	46,0	68,8	23,7	508,8	314,8	8,0	169,0	185,7
31	8,3	43,6	48,1	50,9	40,9	501,4	309,2	9,8	182,0	153,0
32	12,6	43,6	43,8	79,0	15,2	500,5	309,4	8,8	173,0	178,2
33	6,3	52,8	40,9	56,4	34,4	510,2	302,1	8,0	166,0	155,0
34	8,6	43,7	47,8	65,7	24,3	549,9	344,7	11,7	182,0	168,9
35	12,1	44,8	43,1	75,5	17,1	561,5	347,5	13,4	182,0	178,2
36	8,1	49,0	42,9	75,7	17,3	545,4	329,1	12,8	178,0	165,4
37	9,2	40,8	50,0	66,9	23,6	554,4	352,4	10,4	185,0	155,3
38	7,1	44,6	48,3	68,6	22,3	544,8	346,4	10,9	181,0	176,7
39	9,4	47,3	43,4	75,1	17,1	557,4	348,7	12,2	181,0	174,7
40	13,2	34,2	52,7	86,1	9,4	570,4	354,8	11,4	184,0	141,7
41	11,3	30,5	58,2	85,7	9,4	586,4	366,5	7,5	183,0	186,0
42	13,7	39,2	47,1	84,4	10,8	564,4	354,9	9,8	176,0	167,0
43	9,1	32,1	58,8	78,2	16,3	582,9	370,9	8,0	186,0	173,7
44	10,2	30,8	59,1	80,8	14,1	572,5	353,0	8,5	190,0	149,2
45	7,6	33,5	58,8	84,6	10,2	581,9	364,4	12,7	180,0	200,6
46	9,3	24,6	66,1	89,6	5,9	651,7	376,8	9,9	206,0	160,4
47	7,0	22,7	70,3	81,6	11,9	668,7	397,5	9,0	204,0	183,3
48	6,5	24,8	68,7	74,2	17,7	666,6	381,2	8,8	206,0	166,4
49	10,2	55,7	34,1	77,7	16,6	514,2	319,0	15,2	167,0	164,6
50	7,0	51,6	41,4	72,5	19,7	515,7	335,7	8,1	174,0	159,6
51	7,1	45,2	47,7	61,9	27,6	523,9	332,0	10,7	178,0	185,9
Mean	**9.7**	**41.2**	**49.2**	**72.7**	**20.1**	**549.4**	**339.7**	**10.2**	**180.0**	**170.0**
St. Dev.	**2.3**	**9.0**	**9.4**	**10.2**	**8.8**	**50.6**	**26.7**	**1.9**	**11.3**	**13.9**

Table 5. Comparing the CGI and SGI by the mean values of properties

Material	Graphite [%]	Ferrite [%]	Perlite [%]	Grade of nodularity	Grade of Vermicularity	UTS [MPa]	YS [MPa]	ε [%]	HB	E [GPa]
CGI	**13.0**	**61.2**	**25.8**	**16.6**	**81.2**	**337.2**	**267.9**	**3.4**	**144.9**	**149.9**
SGI	**9.7**	**41.2**	**49.2**	**72.7**	**20.1**	**549.4**	**339.7**	**10.2**	**180.0**	**170.0**
Δ	**3.3**	**20**	**-23.4**	**-56.1**	**61.1**	**-212.2**	**-71.8**	**-6.8**	**-35.1**	**-20.1**
%	**34%**	**49%**	**-48%**	**-77%**	**304%**	**-39%**	**-21%**	**-67%**	**-20%**	**-12%**

3.2 Correlation between values

This different mechanical behavior can be related with the specific modality in which the graphite solidified inside the alloy. A better description of the phenomena and their impact on the microstructure is reported in [21, 22] where a deep investigation of fracture behavior for CGI and SGI is proposed by the same authors. In this study, specimens from similar CGI and SGI samples, were mechanically fractured and, then, observed by optical and electron microscopy.

Even without entering in microstructural details, it is possible to related the inhomogeneous tensile properties of specimens to the difference in hardness of the two materials. This difference may be due to the dissimilar perlitic fractions of the matrices . An higher fraction of perlit in SGI, almost double respect to CGI, provides higher hardness, yield strength and ultimate tensile strength values to this material.

In the next Figs., the strict relations between the investigated mechanical properties (as UTS, YS, HB) and the microstructure of alloy (as grade of Graphite, Perlite and Ferrite) is represented, both for SGI and CGI.

In particular, the relation between the Ultimate Tensile Stress (UTS) and the grade (%) of Graphite, Perlite and Ferrite in the alloy is reported in Fig. 8 in the case of SGI. It is evident how UTS is not related to the % of Graphite. On the contrary, the % of Perlite and Ferrite in the microstructure has a direct and proportional influence: while Perlite increases UTS, Ferrite decreases this properties. The same behavior occurs with YS and HB (as shown in Fig. 9).

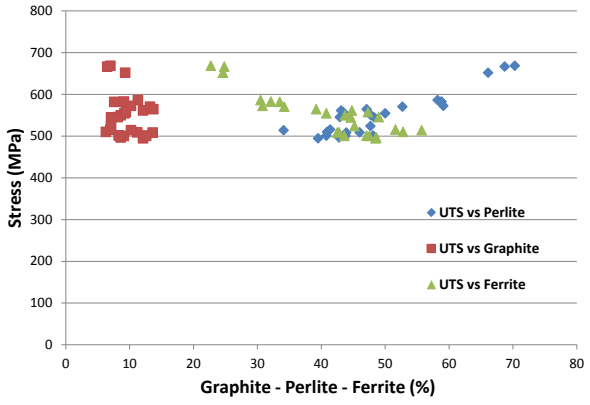

Fig. 8. Relation between the Ultimate Tensile Stress (UTS) of Spheroidal Graphite Iron (SGI) and the grade (%) of Graphite, Perlite and Ferrite.

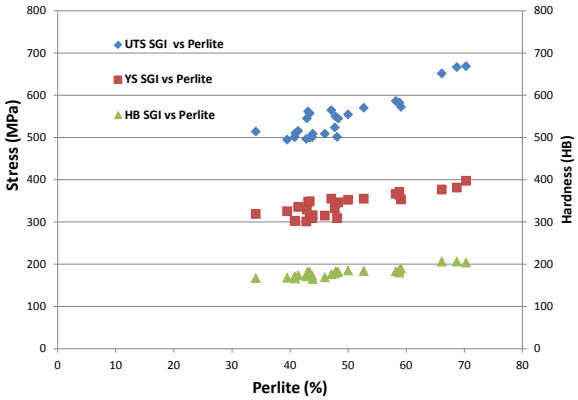

Fig. 9. Relation between the Ultimate Tensile Stress (UTS), Yield Strength (YS) and Hardness (HB) of SGI and the grade (%) of Perlite.

Comparing the behavior of SGI and CGI respect to modifications in the grade of Perlite, in Fig. 10, or in Nodularity, in Fig. 11, it is highlight similar trends, even if with different consistency in variations.

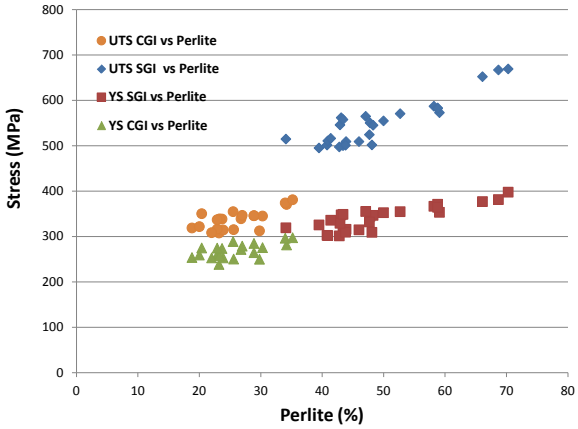

Fig. 10. Comparing UTS and YS for CGI and SGI respect to modifications in the grade (%) of Perlite.

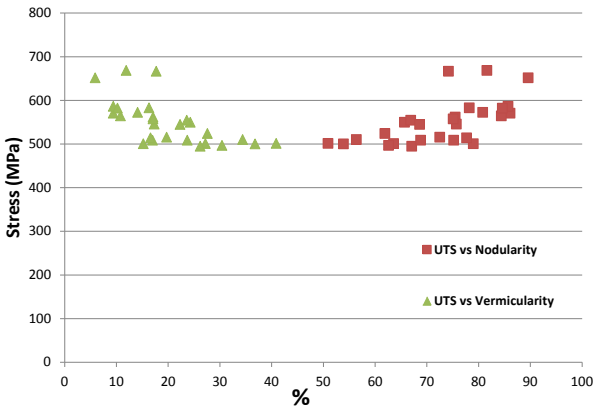

Fig. 11. Relation between UTS of SGI and the grade (%) Nodularity or Vermicularity

3.3 Stress strain curve

Stress-strain curves were carefully evaluated for all specimens. A comparison between stress-strain curves for CGI and SGI, both in terms of *engineering* or *true* stresses, are reported, respectively, in Fig. 12 and 13. Also in this case, experimental data confirm the better mechanical properties offered by SGI respect to CGI. In particular, SGI shows its higher ductility (especially in term of *engineering* stress) with the size of plastic regions more than double.
Additional information from graphs are:

- ✓ Low variability between stress-strain curves inside the same material (it also means a repeatability of experiments);
- ✓ Similar slopes for SGI and CGI (it also means a similar Young's Modulus).

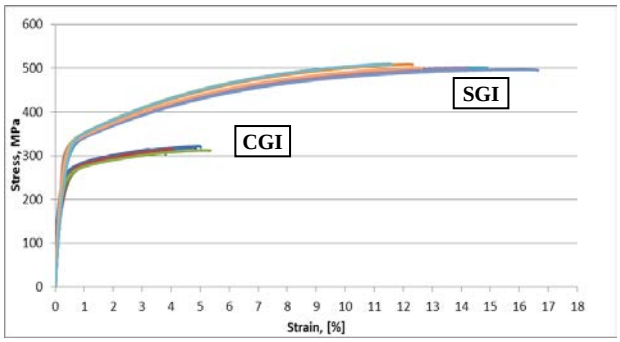

Fig. 12. *Engineering* stress-strain curve for SGI & CGI

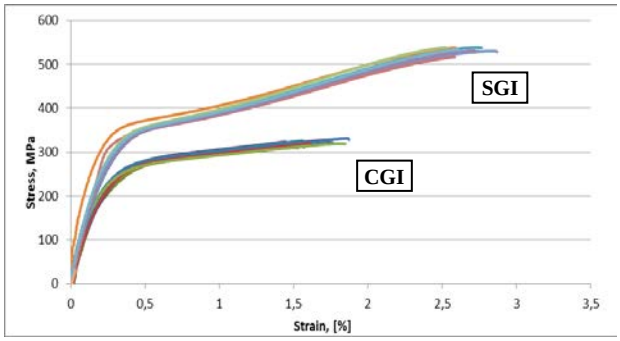

Fig. 13. *True* stress-strain curve SGI and CGI

3.4 Yield Strength

Ductile materials are characterized by their ability to yield at normal temperatures (Fig. 14). They generally exhibits a very linear stress–strain relationship up to a yield point. The linear portion of the curve is the elastic region and the slope is the modulus of elasticity or Young's Modulus (Young's Modulus is the ratio of the compressive stress to the longitudinal strain). After the yield point, the curve typically decreases slightly. As deformation continues, the stress increases on account of strain hardening until it reaches the ultimate tensile stress. Until this point, the cross-sectional area decreases uniformly and randomly because of Poisson contractions. It is often difficult to precisely define yielding due to the wide variety of stress–strain curves exhibited by real materials. Several possible ways to define yielding exist.

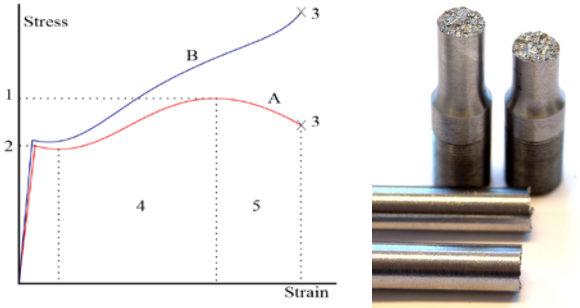

Fig. 14. A stress–strain curve typical of steel. 1: Ultimate strength 2: Yield strength 3: Rupture 4: Strain hardening region 5: Necking region A: Engineering stress; B: Real stress

In this investigation, the *offset yield point* (*proof stress*) was adopted in accordance with [23]: when a yield point is not easily defined with accuracy based on the shape of the stress-strain curve, like in the current case, an offset yield point is arbitrarily defined. According with the standardized application of the method, the value for this offset is set at 0.2% plastic strain.
Specifically, the Yield Strength (YS) for each specimen was evaluated, by a 0.2% offset line, parallel to the initial parts of stress-strain curves, which intersection with the same stress-strain curve, represents the YS point (Fig. 15).

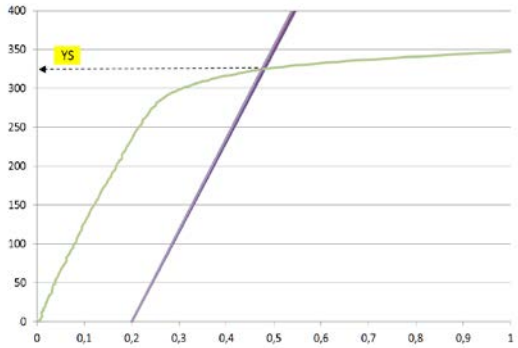

Fig. 15. Determination of Yield Strength (YS) as 0.2% offset line, parallel to the initial part of the stress-strain curve

3.5 True and engineering stress

Engineering stresses versus true stresses were also investigated.
In Tab. 6 a comparison between numerical results that can be obtained using engineering or real stresses is reported. In this case, they are proposed, for instance, in terms of engineering or real Ultimate Tensile Stress (in MPa). A difference of 2.1% and 5.9% is respectively reported for both CGI or SGI. Trends representing the real and engineering stresses in function of deformation are also evident in the previous Fig. 11 and 12. The difference could be up to 30 MPa in case of SGI, while in case of CGI is limited to 10 MPa.

Table 6. Comparing *engineering* and *real* stress in terms of Poisson Modulus in the of CGI and SGI

CGI			SGI		
Specimen	UTS *in MPa*		Specimen	UTS *in MPa*	
	Eng	*True*		*Eng*	*True*
1	318.8	328.1	25	500.0	534.6
2	350.1	354.8	26	501.0	524
3	307.5	317.0	27	508.7	546
4	314.1	321.1	28	496.8	526.8
5	316.2	323.1	29	494.8	528.4
6	308.4	317.6	30	508.8	538.8
7	321.7	330.7	31	501.4	532.7
8	315.0	317.6	32	500.5	534
9	312.4	314.7	33	510.2	541.3
Mean	318.2	325.0	*Mean*	502.5	534.1
Δ	6.7		Δ	31.6	
Δ%	2.1%		Δ%	5.9%	

Entering in details, as previously described, the *engineering stress* is the load divided by this initial cross area, while the *true stress* is the load divided by the cross area at that instant. This area continuously changes during the test since the conservation of mass but, in particular, it changes faster when the yield limit is reached. Before that point, the material is deforming elastically and differences are marginal (in the case of metals).
As a consequence, the difference between the true and engineering stresses, since they are related to changes in specimens respect to the initial geometry, has to be almost negligible during the initial phase of load application. Then, this difference progressively increases, almost linearly, up to the yield stress. Passing this limit, everything changes since the properties of material change: the occurring plasticity provides to deform the material easier than before, including the deformation of the initial cross-section. Then, the difference between engineering and real stress continues to increase, but following a different trend.
These theoretical changes in trends were investigated by experiments and reported in Fig. 15 and 16 for CGI and SGI. Beyond the difference in general values between CGI and SGI it is also evident a larger dispersion of trends in the case of CGI: both situations are related to the lower ductility of CGI respect to SGI.

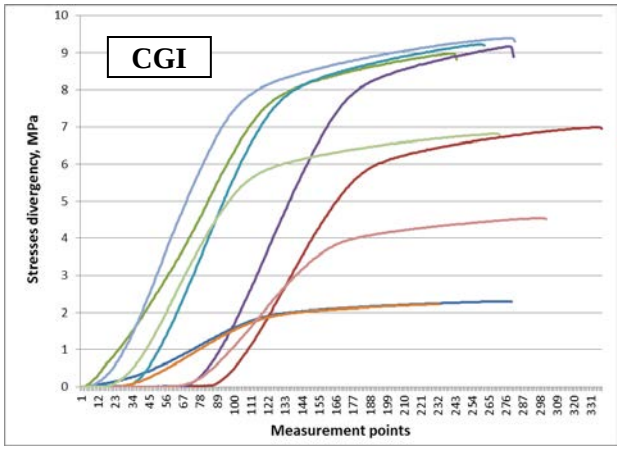

Fig. 15. Divergence between true and engineering stresses in the case of CGI.

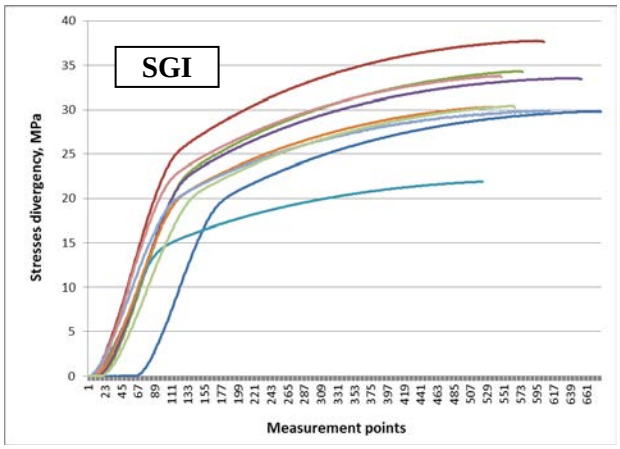

Fig. 16. Divergence between true and engineering stresses in the case SGI.

4. CONCLUSION

The mechanical properties for Compacted Graphite Iron (CGI) and Spheroidal Graphite Iron (SGI) were measured using tensile tests and hardness tests on a large number of specimens. For both alloys it was possible to define the Ultimate Tensile Strength, Yield Strength, Maximal Elongation to Failure, Young's Modulus and Hardness over a large number of specimens. Engineering and true stresses were also considered and compared. Several evidences were remarked about the stress-strain behavior of both materials, including elasticity, plasticity and the transition phase. Additional notes were reported with the aim at investigating the complex relation between the mechanical properties and the peculiarities of the microstructure, described by the grade of Graphite, Perlite, Ferrite, Nodularity, Vermicularity. With additional investigations to be realized over the appearance of round metal bars after tensile testing, it would be possible to understand which kind of fracture, between brittle, partially ductile or completely ductile, occurred and to obtain further useful information. In general, it is important to consider that, although SGI is quite largely investigated material since its wide use, CGI misses deep and definitive studies. A better knowledge on chemical compositions and mechanical properties for CGI is a fundamental step toward its formal classification between the other common cast irons, promoting its larger utilization in industry. Several organizations for standardization are moving in that direction. This analysis has to be considered as part of a larger and more complex investigation aiming at comparing ductile (SGI) and vermicular (CGI) cast irons. Other mechanical properties were also investigated by experiments as fatigue [24], fracture toughness [22], together with their impacts on industrial applicability [25].

Acknowledgement

This research with the contribution of the European Union as part of the IPA Adriatic Cross-Border Cooperation Program. More details in [26].

REFERENCES

[1] F.C. Campbell. *Elements of Metallurgy and Engineering Alloys*. Materials Park, Ohio: ASM International. p. 453, 2008

[2] R. Elliott, *Cast iron technology*. London: Butterworth-Heinemann, 1988.

[3] Sinha, Anil Kumar. *Physical metallurgy handbook*. McGraw-Hill Professional Publishing, 2003.

[4] H. T. Angus. *Cast Iron: Physical and Engineering Properties.* London: Elsevier, 2013.

[5] H. T. Angus, *Physical and Engineering Properties of Cast Iron: A Data Book for Engineers and Designers*. British Cast Iron Research Ass., 1960.

[6] B. Bobic, S. Mitrovic, M. Babic, A. Vencl and I. Bobic, 'Corrosion Behavior of the As-cast and Heat-treated ZA27 Alloy', *Tribology in Industry*, vol. 33, No. 2, pp. 87-93, 2011.

[7] D.G. Mallapur and K.R. Udupa, 'A Comparative Study on Wear Properties of As Cast, Cast Aged and Forge Aged A356 Alloy with Addition of Grain Refiner and/or Modifier', *Tribology in Industry*, vol. 37, no. 1, pp. 81-87, 2015.

[8] I.C.H. Hughes and J. Powell: Compacted Graphite Irons - High quality engineering materials in the cast iron family. In: *SAE Paper* 840772, 1984.

[9] T.L. Anderson. *Fracture mechanics: fundamentals and applications*. CRC press, 2005.

[10] I.C.H. Hughes and J. Powell: Compacted Graphite Irons - High quality engineering materials in the cast iron family. In: SAE Paper 840772, 1984.

[11] J.D. Altstetter and R.M. Nowicki: Compacted Graphite Iron - Its properties and automotive applications. In: AFS Transactions 82-188, pp. 959-970, 1982.

[12] W. C. Lyons and G. J. Plisga. *Standard Handbook of Petroleum & Natural Gas Engineering*, Elsevier, 2006

[13] SCM Foundry, accessed on 15.11.2015 at: http://www.scmfonderie.it/?l=en&p=azienda,

[14] G.E. Dieter and D. Bacon, *Mechanical metallurgy (Vol. 3)*, McGraw-Hill, New York,1986.

[15] E. Roy, *Cast iron technology*. London: Butterworth-Heinemann, 1988.

[16] EN 10002-1: 2001. Metallic materials – Tensile testing – Part 1: Method of test at ambient temperature

[17] EN 1563:2012. Founding. Spheroidal graphite cast iron

[18] I. Minkoff, *The physical metallurgy of cast iron*. New York: Wiley, 1983.

[19] I. Faridmehr, M.H. Osman, A.B. Adnan, A.F. Nejad, R. Hodjati, and M. Azimi, 'Correlation between Engineering Stress-Strain and True Stress-Strain Curve', *American Journal of Civil Engineering and Architecture*, vol. 2, no. 1, pp. 53-59, 2014.

[20] Y. Ling, 'Uniaxial true stress-strain after necking', *AMP Journal of Technology*, Vol. 5, pp. 37-48, 1996.

[21] N. Radović, A. Morri and C. Fragassa, 'A study on the tensile behaviour of spheroidal and compacted graphite cast irons based on microstructural analysis', *11th IMEKO TC15 Youth Symposium on Experimental Solid Mechanics,* 30.05-02.06.2012, Brasov, Romania. pp. 185-190.

[22] C. Fragassa, G. Minak and A. Pavlovic, 'Tribological aspects of cast iron investigated via fracture toughness', *Tribology in Industry*, vol. 38, No. 1, pp.1-10, 2016.

[23] C. Ross, *Mechanics of Solids*, Horwood Pub Albion, 1999

[24] C. Fragassa, R. Zigulic and A. Pavlovic, 'Push-pull fatigue test on ductile and vermicular cast irons', *Engineering Review,* vol. 36, No. 3, 2016.

[25] G. Lucisano, M. Stefanovic and G. Minak, 'Advanced Design Solutions for High-Precision Woodworking Machines', *International Journal for Quality Research,* vol. 10, No. 1, 2016.

[26] M. Savoia, M. Stefanovic, C. Fragassa, 'Merging technical competences and human resources with the aim at contributing to transform the Adriatic area in a stable hub for a sustainable technological development', *International Journal of Quality Research,* vol. 10, no. 1, pp. 1-12, 2016